Cluster formation and bulk phase behavior of colloidal dispersions

Tao Jiang and Jianzhong Wu*
Department of Chemical and Environmental Engineering, University of California, Riverside, California 92521-0444, USA
(Received 20 March 2009; revised manuscript received 22 June 2009; published 10 August 2009)

We investigated cluster formation in model colloids where the interparticle potential beyond the collision diameter includes a short-ranged attraction and a longer-ranged repulsion. The structure and thermodynamic properties of the model system can be accurately described by the first-order mean-spherical approximation (FMSA) and a perturbation theory for bulk phases and by a nonlocal density-functional theory (DFT) for stable/metastable clusters. In corroboration with recent experiments and molecular simulations, we predicted that the bulk to cluster transition may occur at both one-phase and two-phase regions of the colloidal phase diagram. While formation of colloidal clusters appears uncorrelated with the bulk phase transitions, the local phenomena may nevertheless play an important role in the dynamics of stable colloids and the kinetics of colloidal phase transitions.

DOI: 10.1103/PhysRevE.80.021401 PACS number(s): 82.70.Dd, 64.75.Xc, 47.57.J−

I. INTRODUCTION

Recent theoretical and experimental investigations both suggest that various micro/mesoscopic phases may appear in bulk colloidal systems [1–4] or protein solutions [5–8] where the interparticle potential consists of a short-ranged attraction and a longer-ranged repulsion beyond the collision diameter. The short-ranged attraction typically arises from chemical association such as hydrogen bonding and van der Waals attraction while the longer-ranged repulsion may come from solvation forces, polymer-mediated steric repulsion or electrostatic interactions. A competition of the repulsive and attractive components of the colloidal forces leads to formation of lamellar and cluster structures similar to those appeared in a system containing surfactants or block copolymers. While knowledge for the phase behavior of bulk colloids is now well advanced [8–15], much lagged behind are theoretical predictions of the micro/mesoscopic phases and their implications on the kinetics of bulk phase transitions. A full understanding of the colloidal phase behavior is of fundamental importance not only from a theoretical viewpoint but also pertinent to a number of technological applications ranging from colloidal stabilization [16,17] to materials self-assembly [18,19], and crystallization of globular proteins in an aqueous solution [4,20,21].

Colloidal clusters are qualitatively different from aggregates in kinetically destabilized colloids. The clusters are in a thermodynamically stable/metastable state that satisfies a local free-energy minimum; they have distinctive geometric characteristics and a narrow size distribution [3,4,22]. Such well-defined features contrast the nonequilibrium aggregates formed in a thermodynamically unstable colloid that typically have a broad size distribution and fractal internal structures. Apparently, the stable or metastable colloidal clusters are also different from the critical nucleus appeared during vapor-liquid-like condensation or crystallization in a colloidal dispersion [23]. While a critical nucleus appears during the bulk phase transition as a transient state or a saddle point in the free-energy landscape, an equilibrium/metastable cluster satisfies a local free-energy minimum [7]. Besides, clusters may appear both in thermodynamically stable one-phase region and in unstable two-phase regions of the colloidal phase diagram but nucleation is a transient process affiliated only with thermodynamically unstable systems [6]. The existence of clusters in thermodynamically stable systems implies that many colloids and protein solutions may have an intrinsic propensity to form mesoscopic structures with only finite lifetime. Such clusters will have significant implications to understanding the dynamic properties of equilibrium systems and the kinetics of phase transitions.

Formation of colloidal clusters can be intuitively understood in terms of a competition of the short-ranged attraction (favors aggregation) with the longer-ranged repulsion (prohibits of further growth). The force balance argument ignores reduction of the translational entropy of the individual particles and predicts that clusters are formed only at thermodynamically metastable or unstable conditions [7,10]. Recent experiments for protein systems, however, indicate that clusters formed in dilute solutions exhibit no tendency of bulk phase transitions [6]. By using the integral-equation theory [24] and density-functional theory (DFT) [25], Archer and co-workers analyzed the structure and phase behavior of model colloids with competing attractive and repulsive forces and identified a so-called lambda line defined by the divergence of the structure factor at a fine wavelength. The microscopic theories indicate the propensity of colloids toward clustering but the divergence of structure factor occurs only at thermodynamically unstable conditions. Besides, the integral-equation methods are not reliable for nonequilibrium systems and thus the connection of lambda line to cluster formation is not immediately obvious. To our knowledge, no theoretical investigations have been reported on the formation of clusters in thermodynamically stable systems. A reliable theoretical method is yet to be established for identification of thermodynamic conditions favoring cluster formation. While colloidal clusters are expected only at appropriate conditions where the short-ranged interparticle attraction and the long-ranged repulsion reach a delicate balance [13,26], little investigations have been reported examining the details of how the balance of the opposite

*jwu@engr.ucr.edu

colloidal interactions affects cluster size and stability.

In this work, we investigate formation of spherical clusters in dilute colloidal dispersions that are thermodynamically stable or metastable. Formation of mesoscopic colloidal structures at higher concentrations has been reported in a previous publication [27]. As before, a double-Yukawa potential is used to represent the interparticle interactions in which the relative range and strength of attraction and repulsion can be conveniently controlled by changing the model parameters. We demonstrated in a number of previous publications that the structure and thermodynamic properties of the model system can be reliably described by a combination of the first-order mean-spherical approximation (FMSA) for bulk fluids, a first-order perturbation theory (FPT) for bulk solids, and a nonlocal DFT for inhomogeneous systems [28–32]. We expect that these theoretical methods are reliable for understanding cluster formation and its implications to the bulk fluid-fluid and fluid-solid transitions. Although this work is confined to formation of spherical clusters, the same theoretical tools will allow us to examine the size and structure of other mesoscopic structures over a broad range of the parameter space [1,15]. While cluster formation in a thermodynamically stable system may have little influence on the bulk phase transitions, its appearance under unstable/metastable regions of the phase diagram will have significant implications on the kinetic pathways of macroscopic phase transitions.

The remainder of this article is organized as follows. Section II describes briefly the molecular model and formulation of theoretical methods for representing the structure and thermodynamic properties of the bulk and inhomogeneous phases. In Sec. III, we investigate cluster formation and bulk phase diagram of the model colloidal systems. The emphasis is placed at the effects of the interaction strength and range of intercolloidal forces on the size and internal structure of equilibrium clusters and their distribution in the bulk phase diagrams. For comparison, the free-energy landscape of nucleation in the Lennard-Jones fluids is also investigated in which the interaction energy can also be effectively represented by the double-Yukawa potential. Section IV summarizes the main results and discussions.

II. MOLECULAR MODELS AND THEORIES

For a quantitative and self-consistent description of the bulk fluid-fluid, fluid-solid phase equilibria and cluster formation in a colloidal system, we limit our interest to an idealized model colloid where the interparticle potential consists of a short-ranged attraction and a longer-ranged repulsion

$$\beta U(r) = \begin{cases} \infty, & r < \sigma \\ \varepsilon^* \left\{ -\dfrac{\exp[-Z_A(r/\sigma - 1)]}{r/\sigma} + \lambda \dfrac{\exp[-Z_R(r/\sigma - 1)]}{r/\sigma} \right\}, & r \geq \sigma \end{cases}, \tag{1}$$

where r stands for the center-to-center distance between two spherical particles, σ is the particle diameter. In Eq. (1), ε^* is a dimensionless energy parameter reflecting the strength of the potential, parameter λ provides a measure of the relative strength of the repulsion, parameters Z_A and Z_R control the ranges of attraction and repulsion, respectively, and $\beta = 1/k_BT$ with k_B being the Boltzmann constant and T the absolute temperature. The double-Yukawa potential mimics the classical Derjaguin-Landau-Verwey-Overbeek (DLVO) theory for typical colloidal interactions in an aqueous environment. The model parameters in Eq. (1) depend implicitly on the solvent and solution conditions. While the one-component model drastically simplifies the chemical complexity of colloids or protein solutions, it is sufficient to capture the essential feature of cluster formation and its interplay with the colloidal phase diagrams. Throughout this work, we fix $Z_A = 3$ so that the range of attraction is roughly 30% of the particle diameter. The range of repulsion varies and spans up to around several times the particle diameter.

It has been demonstrated in a number of previous publications that the thermodynamic properties of the double-Yukawa system can be accurately represented by a first-order mean-spherical approximation for bulk fluids, by a first-order perturbation theory for a bulk solid, and by a nonlocal density-functional theory for inhomogeneous systems [28–32]. In particular, the DFT provides a unified theoretical framework to describe both bulk and inhomogeneous phases because for a uniform system, it reduces to an equation of state or an expression for the Helmholtz free energy identical to that from the FMSA. While the DFT is also applicable to the solid phase, the FPT suffices in representing the thermodynamic properties of interest in this work. The different theoretical framework for the solid phase has little consequence on cluster formation at dilute solutions.

According to the DFT, the Helmholtz energy functional for a double-Yukawa system can be formally expressed as

$$F = F^{id} + F^{hs} + F^{DY}, \tag{2}$$

where F^{id} corresponds to that for an ideal gas at the system temperature and number density, F^{hs} accounts for thermodynamic nonideality due to the hard-core repulsion, and F^{DY} represents contributions to the Helmholtz energy due to the double-Yukawa potential. The ideal-gas term is known exactly

$$\beta F^{id} = \int d\mathbf{r} \rho(\mathbf{r}) [\ln \rho(\mathbf{r}) - 1], \tag{3}$$

where $\rho(\mathbf{r})$ stands for the local number density distribution of colloidal particles. In Eq. (3), we omit the thermal wave-

length because it makes no contribution to phase-equilibrium calculations.

As detailed in our previous publications [28–32], the excess Helmholtz energy due to the hard-core repulsion is represented by a modified fundamental measure theory (FMT)

$$\beta F^{HS} = \int d\mathbf{r}\left\{ -n_0 \ln(1-n_3) + \frac{n_1 n_2 - \mathbf{n_{V1}}\mathbf{n_{V2}}}{1-n_3} + \frac{1}{36\pi}\left[\ln(1-n_3) + \frac{n_3}{(1-n_3)^2}\right]\frac{(n_2^3 - 3n_2\mathbf{n_{V2}}\mathbf{n_{V2}})}{n_3^2}\right\}, \quad (4)$$

where $n_\alpha(\mathbf{r})$, $\alpha=0,1,2,3,\mathbf{V1},\mathbf{V2}$ are scalar and vector weighted densities from the FMT [33]. The excess Helmholtz energy due to the double-Yukawa potential is derived from a quadratic expansion of the free energy with respect to that at the local density

$$\beta F^{DY} = \beta \int d\mathbf{r}\rho(\mathbf{r}) f^{DY}(\mathbf{r}) + \frac{1}{4}\int\int d\mathbf{r}d\mathbf{r}'\Delta C^{DY}(|\mathbf{r}-\mathbf{r}'|,\bar{\rho}) \times [\Delta\rho(\mathbf{r},\mathbf{r}')]^2, \quad (5)$$

where $f^{DY}(\mathbf{r})$ and $\Delta C^{DY}(r,\bar{\rho})$ represent, respectively, the local excess Helmholtz energy per particle and the direct correlation function in the fluid phase due to the double-Yukawa potential; $\bar{\rho}=[\rho(\mathbf{r})+\rho(\mathbf{r}')]/2$; $\Delta\rho(\mathbf{r},\mathbf{r}')=\rho(\mathbf{r})-\rho(\mathbf{r}')$. Equation (5) is derived from a uniform density approximation for the direct correlation function of the inhomogeneous system and corresponding bulk fluid [34]. The expressions for f^{DY}, $\Delta C^{DY}(r,\bar{\rho})$, and $n_\alpha(\mathbf{r})$ are given in previous publications [28,29,35].

Colloidal clusters can be identified by minimization of the grand potential

$$\Omega[\rho(\mathbf{r})] = F[\rho(\mathbf{r})] - \mu\int d\mathbf{r}\rho(\mathbf{r}), \quad (6)$$

where μ stands for the chemical potential of colloidal particles. As a result, the density profile of colloidal particles satisfies the Euler-Lagrange equation

$$\rho(\mathbf{r}) = \exp\left[\beta\mu - \frac{\delta\beta F^{ex}}{\delta\rho(\mathbf{r})}\right], \quad (7)$$

with $\beta F^{ex}=\beta F^{hs}+\beta F^{DY}$. Equation (7) is solved by using the Picard iteration method with a step function as the initial guess

$$\rho(r) = \begin{cases} \rho_L, & r \le r_0 \\ \rho_H, & r > r_0 \end{cases}, \quad (8)$$

where r_0 is the initial cluster radius, ρ_L and ρ_H are initial densities outside and inside the cluster. During the Picard iteration, we evaluate the effective one-body potential

$$\lambda(r) = \frac{\delta F^{ex}}{\delta\rho(r)} \quad (9)$$

and from which a new set of density profile is obtained by using Eq. (7). The new density profile is then mixed with the previous result to feed the next iteration. The final result is achieved when the overall difference between the input and output density profiles is less than 1×10^{-6} in reduced units $(\rho\sigma^3)$.

For a bulk fluid, the particle density is everywhere identical. Consequently, Eq. (2) reduces to an equation of state for the Helmholtz energy

$$\beta F/V = \rho_b(\ln\rho_b - 1) + \beta\rho_b f^{DY} - n_0\ln(1-n_3) + \frac{n_1 n_2}{1-n_3} + \frac{n_2^3}{36\pi n_3^2}\left[\ln(1-n_3) + \frac{n_3}{(1-n_3)^2}\right], \quad (10)$$

where ρ_b stands for the bulk density, f^{DY} is the Helmholtz energy density for a bulk system calculated from the FMSA, and the n_α-dependent terms are the same as those from the Boublik-Mansoori-Carnahan-Starling-Leland (BMCSL) equation of state [36,37].

The thermodynamic properties of the bulk solid can be quantitatively described by a first-order perturbation theory [31]. Within the parameters investigated in this work, the double-Yukawa system forms a face-centered-cubic (FCC) solid at sufficiently high particle density. Similar to that for a bulk fluid, the Helmholtz energy of the solid includes a term accounting for a reference FCC hard-sphere crystal and a perturbation arising from the double-Yukawa potential

$$\beta F/N = \beta F^{HS}/N + 12\eta\sigma^{-3}\int r^2 g_S^{HS}(r)\beta U(r)dr, \quad (11)$$

where βF^{HS} is the Helmholtz energy of the hard-sphere solid at system packing density, $g_S^{HS}(r)$ is the radial distribution function of the hard-sphere solid, and $\beta U(r)$ is the interparticle potential given by Eq. (1). The Helmholtz energy of the hard-sphere solid is given by a modified cell model, and the radical distribution function of FCC hard spheres is represented by a summation of an empirical exponential function for the nearest neighbors and parameterized Gaussian distributions in the remaining layers. The detailed expressions of βF^{HS} and $g_S^{HS}(r)$ can be found in our previous publication [31].

III. RESULTS AND DISCUSSION

Colloidal clusters are thermodynamically stable or metastable relate to the uniform phase. The microscopic structure of each cluster can be directly identified by minimization of the free-energy functional. The minimization process makes cluster calculation computationally simpler than identification of the critical nucleus for a bulk phase transition. However, even for a system of spherically symmetric particles, the colloidal clusters may exhibit complicated three dimensional structures. In this work, we focus only on spherical clusters and assume that the cluster structure can be represented by a spherically symmetric density profile.

Figure 1 presents typical density profiles in colloidal clusters identified by the DFT calculations. Here the range parameter is fixed as $Z_R=1$, the reduced temperature is $k_bT/\varepsilon_A=0.3333$, and $\lambda=0.2$. In this case, the equilibrium cluster is formed only when the bulk density is higher than $\rho_b\sigma^3=0.075$. The discontinuous jump of cluster size at

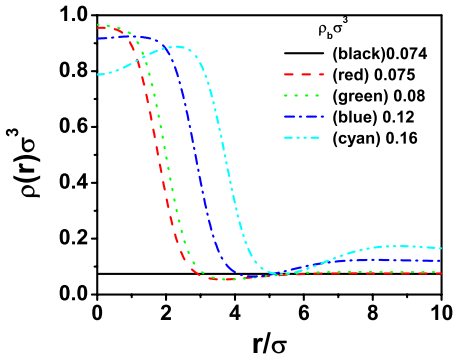

FIG. 1. (Color online) Density profiles of colloidal clusters represented by a double-Yukawa potential. No cluster is formed for the colloidal density smaller than $\rho_b\sigma^3=0.074$. For $\rho_b\sigma^3\geq 0.075$, cluster formation is identified at $k_bT/\varepsilon_A=0.3333$, $\lambda=0.2$, with $Z_A=3$ and $Z_R=1$.

$\rho_b\sigma^3=0.075$ suggests cluster formation follows a first-order-like phase transition. Below the critical transition density, no cluster is formed and the system exhibits only a uniform density distribution. Beyond the transition density, the cluster size increases smoothly with the average bulk density. The density profile spans $2\sim 5\sigma$ from the cluster center and exhibits by a weak depletion layer near the cluster surface. The slight increase of the cluster radius with the bulk density is accompanied by a reduction of the peak density near the center.

Figure 2 shows the dependence of the cluster size on the average bulk density. The cluster size Δn is defined as an excess relative to a uniform system of density ρ_b,

$$\Delta n = \int [\rho(r) - \rho_b] \cdot 4\pi r^2 dr. \tag{12}$$

Here, the different curves correspond to cluster formation at different temperatures (k_bT/ε_A) but with the same set of energy parameters ($\lambda=0.2$, $Z_A=3$, and $Z_R=1$). As observed in colloidal experiments [2], the clusters grow in size upon increasing the packing fraction. This contrasts cluster formation in some protein solutions where the cluster size is a weak function of the protein concentration [6]. The difference arises probably from the intrinsic amphiphilic anisotropy of the protein surface. We find that equilibrium clusters appear only in a narrow range of the reduced temperature $0.25\leq k_bT/\varepsilon_A\leq 0.4$. Outside this region, that is, when $k_bT/\varepsilon_A\leq 0.25$ or $k_bT/\varepsilon_A\geq 0.4$, no stable cluster can be identified. Within the range of temperature that clusters are formed, the colloidal system exhibits a first-order-like cluster transition, as manifested by the discontinuity in the cluster formation "isotherms." Interestingly, the discontinuity in cluster size resembles that in a prewetting transition of a simple fluid near at a solid substrate where the liquid-film thickness changes discontinuously with the bulk density [38].

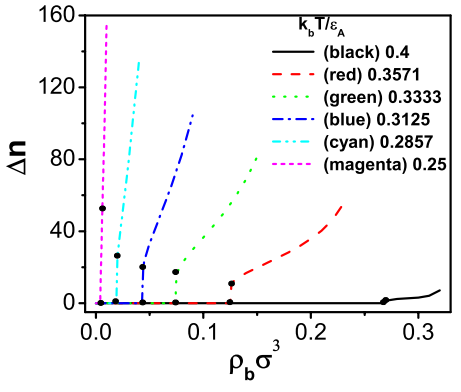

FIG. 2. (Color online) Cluster formation isotherms at different reduced temperatures (k_bT/ε_A), with $\lambda=0.2$, $Z_A=3$, and $Z_R=1$. Black points indicate the cluster transition jumps.

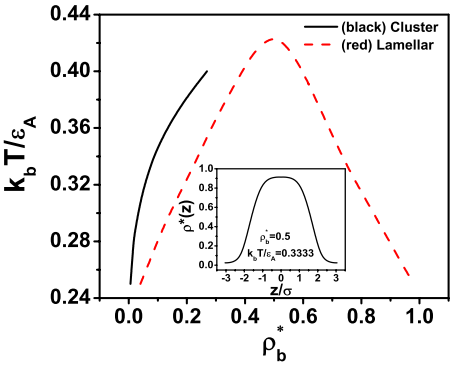

FIG. 3. (Color online) Phase diagram for the cluster and lamellar transitions with $\lambda=0.2$, $Z_A=3$, and $Z_R=1$. Inset: density profiles within the lamellar phase for $k_bT/\varepsilon_A=0.3333$ and $\rho_b\sigma^3=0.5$.

For most systems considered in this work, the clusters are thermodynamically stable, i.e., the cluster formation boundary is located at the stable region of the phase diagram. We find that a decrease of the temperature favors cluster formation, i.e., the equilibrium cluster appears at a lower bulk density but with a larger size. On the other hand, as indicated in Figs. 1 and 2, at a given temperature, an increase of the bulk density results in formation of clusters of larger sizes. Moreover, cluster formation "isotherms" stop at a sufficiently high bulk density, beyond which the DFT calculations cannot reach the convergence. In this case, we expect that the system will form mesoscopic structures other than the spherically symmetric geometry, for example, a lamellar structure. To test our conjecture, we include the calculated results for lamellar structures under the same conditions as those used in Figs. 1 and 2. The calculations of lamellar structures are performed at the planar geometry by assuming that the average density equals to the bulk density. As shown in Fig. 3, the cluster boundary is located at the low-density side of lamellar boundary. At sufficiently large bulk density, the system enters into the lamellar region where the lamellar structure is thermodynamically more stable than the cluster structure. As shown in the inset, the microstructure of a typical lamellar phase exhibits alternating condense and dilute layers.

Figure 4 presents the reduced excess grand potential $\Delta\Omega$ as a function of the cluster size for the same systems as described in Fig. 2. The excess grand potential $\Delta\Omega$ is defined as

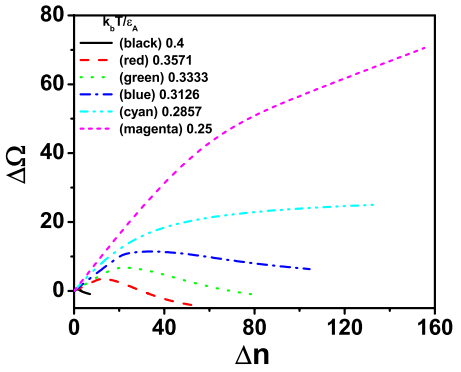

FIG. 4. (Color online) Excess grand potentials of colloidal clusters at different temperatures (k_bT/ε_A) with $\lambda=0.2$, $Z_A=3$, and $Z_R=1$.

$$\Delta\Omega = \Omega[\rho(r)] - \Omega[\rho_b], \tag{13}$$

where $\Omega[\rho(r)]$ represents the free energy of the inhomogeneous system, and $\Omega(\rho_b)$ corresponds to that of the same system with a uniform density distribution ρ_b. At all temperatures, the excess grand potentials are larger than zero for small clusters or equivalently, at low bulk densities. At low-temperatures ($k_bT/\varepsilon_A < 0.31$), the grand potential increases monotonically as the cluster grows, implying that the clusters are metastable. For temperatures $k_bT/\varepsilon_A \geq 0.31$, the grand potential reaches a maximum when the cluster size is sufficiently large. In this case, the excess grand potential can be further reduced to below zero, indicating that the clusters become thermodynamically stable. When comparing the clusters with the same size at different temperatures, the clusters are less stable at lower temperatures. Moreover, reduction of temperature also helps formation of clusters with larger size.

To examine the interplay between cluster formation and bulk phase transitions, we calculated the bulk phase diagrams of the model system based on the FMSA for the fluid-fluid coexistence and the FPT for the fluid-solid coexistence. Figure 5 shows the phase diagrams of the double-Yukawa system at four different relative strengths of the repulsion, including the bulk phase diagrams and the boundary of the cluster transition. Here the ranges of the attraction and repulsion are fixed at $Z_A=3$ and $Z_R=1$, respectively. As shown in Fig. 4, the clusters can be thermodynamically stable or metastable relative to the uniform system, depending on the cluster size, temperature and the range of interparticle potential. The cluster formation boundary reflects conditions in which a colloidal cluster may appear in the bulk fluid. When the clusters appear in the two-phase region of bulk phase transitions, formation of such stable or metastable clusters will affect the kinetics of phase separation. When the interparticle repulsion is relatively weak ($\lambda=0.18$), the phase diagram includes a triple point (dashed line) slightly lower than the critical temperature. At the triple point, three bulk phases, i.e., a dilute solution, a concentrated solution and a crystalline solid are at equilibrium. As the strength of interparticle repulsion increases, the fluid-fluid coexistence curve shifts underneath the fluid-solid lines, indicating that fluid-fluid

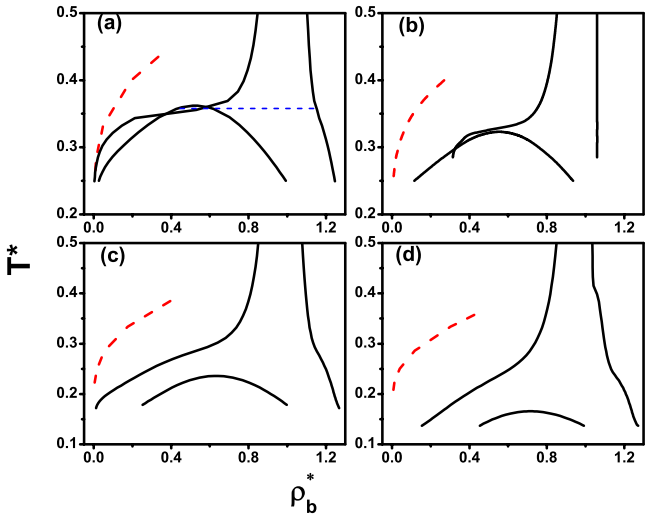

FIG. 5. (Color online) Phase diagram for the cluster formation, bulk fluid-fluid and fluid-solid transitions at (a) $\lambda=0.18$, (b) $\lambda=0.2$, (c) $\lambda=0.25$, and (d) $\lambda=0.3$ with $Z_A=3$ and $Z_R=1$. The smooth curves (black) represent the bulk fluid-fluid and fluid-solid transitions, and the dashed line (red) marks the boundary of the cluster transition.

transition becomes metastable. At all conditions investigated in this work, the cluster boundaries are located at the regions to the low-density (left) side of both the fluid-fluid and fluid-solid coexistence curves. Colloidal clusters are formed upon crossing the cluster formation boundary, i.e., either by lowering the temperature or by increasing the bulk density. Because these clusters are typically metastable, i.e., their free energy is higher than that of the uniform fluid, they are not be able to grow to a macroscopic phase and may return to the uniform phase spontaneously. The cluster region does not span the entire area because the relative cohesive energy decreases with the particle density and the clusters stop to exist beyond a critical value. As stated earlier, it appears that the ends of cluster curve are not directly related to the bulk phase diagram. The cluster formation boundaries are not terminated by the bulk phase transitions. Instead, they are determined by a local free-energy minimum identified by numerical solutions of the Euler-Lagrange equation. The cluster disappears at low density due to unfavorable entropy of nucleation and at high density, due to the decrease of relative cohesive energy or formation of alternative phase (e.g., lamellae). The cluster formation boundary intersects with the fluid-fluid, fluid-solid coexistence curves at $\lambda=0.18$, which coincides with the repulsion limit of cluster formation. We conjecture that in this case, the bulk fluid-fluid or fluid-solid phase transition inhibits the formation of colloidal clusters.

Figure 6 shows the dependence of the cluster size on the temperature and on the relative strengths of the interparticle repulsion. Here the critical cluster is referred to as the cluster formed at the lowest particle density. For all parameters considered in this work, the size of the critical cluster decreases monotonically with the temperature. The trend can be explained by the fact that there are two competing forces represented by the double-Yukawa potential: while the interparticle attraction favors cluster formation, the interparticle

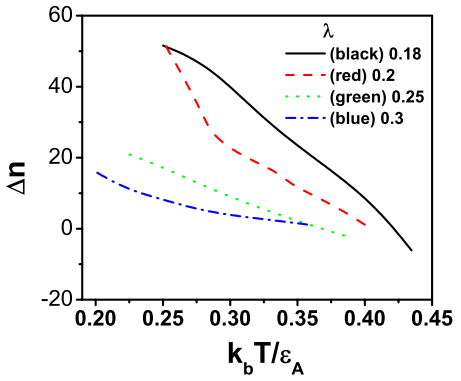

FIG. 6. (Color online) Effect of temperature on the critical cluster size at different λ with $Z_A=3$ and $Z_R=1$.

repulsion tends to disperse the aggregating particles. Whereas an increase of temperature abates both the attraction and repulsion strengths, the magnitude of reduction is more significant for the attraction energy, suggesting that an increase in temperature is unfavorable for cluster formation. At a fixed temperature or equivalently the relative attraction strength, the cluster size decreases with λ due to the repulsive forces. Moreover, an increase of the repulsion strength tends to move the cluster formation toward lower temperature. Interestingly, the width of the temperature range favorable for cluster formation is approximately the same for various strengths of interparticle repulsion.

Figure 7 shows the phase diagrams of bulk double-Yukawa fluids, solids and cluster formations at different ranges of interparticle repulsion. Here two different ranges of repulsion are considered, $Z_R=0.8$ and $Z_R=1.2$, for the long-ranged and short-ranged repulsions, respectively. Figure 7(a) shows the phase diagram of the system with a larger range of repulsion ($Z_R=0.8$). In this case, no stable fluid-fluid-phase equilibrium can be identified, i.e., the critical points of the bulk fluid-fluid transition lies beneath the freezing line. On the other hand, the cluster boundary is located on the lower-density side of the fluid-solid coexistence curve. As the range of interparticle repulsion decreases ($Z_R=1$ and 1.2), the fluid-fluid coexistence curve shifts upward and crosses the fluid-solid coexistence curve (Fig. 7(b) and 7(c)). As a result, a triple point can be identified. The bulk fluid-fluid, fluid-solid, and cluster boundaries intersect when $Z_R=1.2$. Beyond $Z_R=1.2$ no colloidal cluster can be identified because in this case, the cluster formation is deferred by the bulk vapor-liquid transition, similar to that shown in Fig. 4(a).

The thermodynamic model for cluster formation discussed above is equally applied to identification of unstable clusters as appeared in a vapor-liquid-like nucleation. Indeed, by a careful selection of the interaction range and strength parameters, a double-Yukawa potential can mimic the Lennard-Jones (LJ) potential. As shown in previous work [28,29,35], the mapping is optimized by setting the range of interactions as $Z_A=2.90274$ and $Z_R=13.7284$. The numerical performance of the DFT has been tested by direct comparison with Monte Carlo simulations for both bulk and for inhomogeneous van der Waals fluids [28,29,35]. Figure 8 shows a typical free-energy landscape of vapor-liquid nucleation for a van der Waals fluid as represented by a specific double-Yukawa potential. Similar to cluster calculation, the free-energy landscape is directly obtained from iteration by using different initial guesses of the nucleus size (r_0) at $k_bT/\sigma=0.741$ and $\rho_b\sigma^3=0.02$. Here the energy parameters are set as $\varepsilon_A=3.179954$ and $\varepsilon_R=3.9916545$, respectively, obtained by fitting to the LJ potential. Because the critical nucleus represents a saddle point in the free-energy landscape, a unique free-energy path can be identified for the shrinkage ($r_0\leq 2.68\sigma$) and growth ($r_0\geq 2.69\sigma$) of the nuclei.

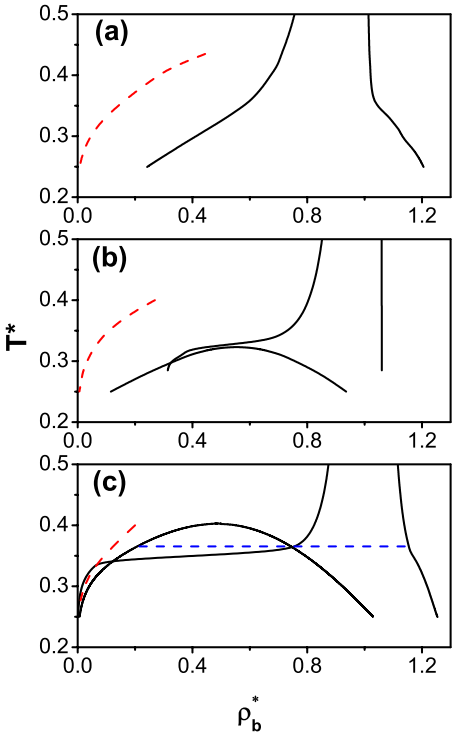

FIG. 7. (Color online) Phase diagram for the cluster formation, bulk fluid-fluid, and fluid-solid transitions at (a)$Z_R=0.8$, (b) $Z_R=1$, and (c) $Z_R=1.2$ with $Z_A=3$ and $\lambda=0.2$. The smooth curves (black) represent the bulk fluid-fluid and fluid-solid transitions, and the dashed line (red) marks the boundary of the cluster transition.

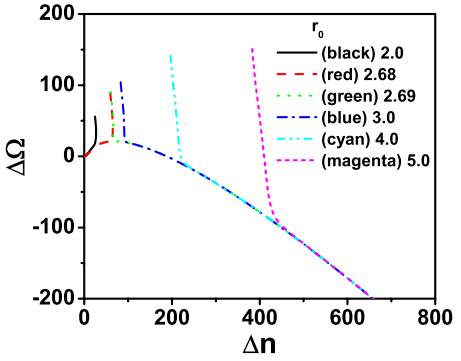

FIG. 8. (Color online) Free-energy landscape of a vapor-liquid-like nucleation obtained by using different initial guesses of the nucleus radius r_0. Here $\rho_b\sigma^3=0.021$, $\varepsilon_A=3.179954$, $\varepsilon_R=3.9916545$, $Z_A=2.90274$, and $Z_R=13.7284$.

IV. CONCLUSIONS

We investigated cluster formation in colloidal dispersions by using a double-Yukawa model and a nonlocal density-functional theory. The thermodynamic properties of the bulk phases are described by a first-order mean-spherical approximation for the fluid phase and a first-order perturbation theory for the solid. By investigating the model system in a broad range of parameter space, we demonstrated that stable or metastable clusters can be formed due to a competition of the short-ranged attraction and longer-ranged repulsion.

Formation of colloidal clusters has been reported in a number of recent experiments and simulations [2,4,12,39]. While previous work was mainly focused the metastable region of the colloidal phase diagram, we demonstrated that stable/metastable clusters may appear also at low densities free of the macroscopic phase transitions. Our calculation explains observation of protein clusters at low concentration and a weak dependence of the cluster radius on the concentration [6].

The fluid to cluster transition resembles a first-order prewetting transition of a vapor near a solid surface. Instead of discontinuity in the liquid-film thickness, discontinuities in the cluster size and microscopic structures can be identified at the critical cluster formation density. Beyond the critical cluster formation density, the equilibrium cluster grows continuously with the average particle density in the bulk. However, the cluster stops to exist at sufficiently large bulk density due to instability condition generated by the bulk phase transition or existence of more stable nonspherical mesoscopic structures.

We discussed cluster formation in the context of the bulk phase diagrams of the double-Yukawa model that exhibits both the bulk fluid-fluid and fluid-solid phase transitions. Within the parameters discussed in this work, the cluster boundaries are always located at densities below both the fluid-fluid and fluid-solid coexistence curves. A reduction of the strength or range of interparticle repulsion leads to convergence of the fluid-fluid, fluid-solid, and cluster transition boundaries and the termination of cluster formation.

ACKNOWLEDGMENTS

This work is supported by the U.S. Department of Energy (Grant No. DE-FG02-06ER46296) and by the National Energy Research Scientific Computing Center (NERSC) under Contract No. DE-AC03-76SF0009. J.W. is grateful to S. Dietrich and his colleagues for hosting his visit of the Max Planck Institute at Stuttgart supported by the Humboldt Foundation.

[1] R. Sanchez and P. Bartlett, J. Phys.: Condens. Matter **17**, S3551 (2005).
[2] A. I. Campbell, V. J. Anderson, J. S. van Duijneveldt, and P. Bartlett, Phys. Rev. Lett. **94**, 208301 (2005).
[3] H. Sedgwick, S. U. Egelhaaf, and W. C. K. Poon, J. Phys.: Condens. Matter **16**, S4913 (2004).
[4] A. Stradner, H. Sedgwick, F. Cardinaux, W. C. K. Poon, S. U. Egelhaaf, and P. Schurtenberger, Nature (London) **432**, 492 (2004).
[5] W. C. Pan, O. Galkin, L. Filobelo, R. L. Nagel, and P. G. Vekilov, Biophys. J. **92**, 267 (2007).
[6] P. G. Vekilov, Ann.. N. Y. Acad. Sci. **1161**, 377 (2009).
[7] S. B. Hutchens and Z. G. Wang, J. Chem. Phys. **127**, 084912 (2007).
[8] A. J. Archer, D. Pini, R. Evans, and L. Reatto, J. Chem. Phys. **126**, 014104 (2007).
[9] R. P. Sear and W. M. Gelbart, J. Chem. Phys. **110**, 4582 (1999).
[10] J. Groenewold and W. K. Kegel, J. Phys. Chem. B **105**, 11702 (2001).
[11] A. Imperio and L. Reatto, J. Chem. Phys. **124**, (2006).
[12] F. Sciortino, S. Mossa, E. Zaccarelli, and P. Tartaglia, Phys. Rev. Lett. **93**, 055701 (2004).
[13] S. Mossa, F. Sciortino, P. Tartaglia, and E. Zaccarelli, Langmuir **20**(, 10756 (2004).
[14] G. J. Pauschenwein and G. Kahl, Soft Matter **4**, 1396 (2008).
[15] A. de Candia, E. Del Gado, A. Fierro, N. Sator, M. Tarzia, and A. Coniglio, Phys. Rev. E **74**, 010403 (2006).
[16] V. Gopalakrishnan and C. F. Zukoski, Phys. Rev. E **75**, 021406 (2007).
[17] S. H. Chen, M. Broccio, Y. Liu, E. Fratini, and P. Baglioni, J. Appl. Crystallogr. **40**, S321 (2007).
[18] A. V. Tkachenko, Phys. Rev. Lett. **89**, 148303 (2002).
[19] Y. Saado, T. Ji, M. Golosovsky, D. Davidov, Y. Avni, and A. Frenkel, Opt. Mater. **17**, 1 (2001).
[20] A. Shukla, E. Mylonas, E. Di Cola, S. Finet, P. Timmins, T. Narayanan, and D. I. Svergun, Proc. Natl. Acad. Sci. U.S.A. **105**, 5075 (2008).
[21] F. Cardinaux, A. Stradner, P. Schurtenberger, F. Sciortino, and E. Zaccarelli, EPL **77**, 48004 (2007).
[22] P. N. Segre, V. Prasad, A. B. Schofield, and D. A. Weitz, Phys. Rev. Lett. **86**, 6042 (2001).
[23] Z. D. Li and J. H. Wu, Ind. Eng. Chem. Res. **47**, 4988 (2008).
[24] A. J. Archer and N. B. Wilding, Phys. Rev. E **76**, 031501 (2007).
[25] A. J. Archer, C. Ionescu, D. Pini, and L. Reatto, J. Phys.: Condens. Matter **20**, 415106 (2008).
[26] R. P. Sear, S. W. Chung, G. Markovich, W. M. Gelbart, and J. R. Heath, Phys. Rev. E **59**, R6255 (1999).
[27] Z. D. Li and J. Z. Wu, J. Chem. Phys. **130**, 165102 (2009).
[28] Y. P. Tang and J. Z. Wu, Phys. Rev. E **70**, 011201 (2004).
[29] Y. P. Tang, J. Chem. Phys. **123**, 204704 (2005).
[30] Y. P. Tang and B. C. Y. Lu, AIChE J. **43**, 2215 (1997).
[31] D. Fu, Y. G. Li, and J. Z. Wu, Phys. Rev. E **68**, 011403 (2003).
[32] D. Fu and J. Z. Wu, Mol. Phys. **102**, 1479 (2004).
[33] Y. Rosenfeld, Phys. Rev. Lett. **63**, 980 (1989).
[34] C. Ebner and W. F. Saam, Phys. Rev. Lett. **38**, 1486 (1977).

[35] Y. P. Tang and J. Z. Wu, J. Chem. Phys. **119**, 7388 (2003).
[36] T. Boublik, J. Chem. Phys. **53**, 471 (1970).
[37] G. A. Mansoori, N. F. Carnahan, K. E. Starling, and T. W. Leland, J. Chem. Phys. **54**, 1523 (1971).
[38] P. Bryk, K. Bucior, S. Sokolowski, and G. Zukocinski, J. Phys. Chem. B **109**, 2977 (2005).
[39] F. Sciortino, P. Tartaglia, and E. Zaccarelli, J. Phys. Chem. B **109**, 21942 (2005).